Hindawi
Advances in Civil Engineering
Volume 2020, Article ID 1898953, 19 pages
https://doi.org/10.1155/2020/1898953

Research Article

Prediction Model of Minimum Void Ratio for Various Sizes/Shapes of Sandy Binary Mixture

Chaojie Shen, Zhaoyang Xu, Jie Yin, and Jinfeng Wu

College of Civil Science and Engineering, Yangzhou University, Yangzhou 225127, China

Correspondence should be addressed to Zhaoyang Xu; 1043073680@qq.com

Received 20 February 2020; Revised 25 May 2020; Accepted 12 June 2020; Published 30 June 2020

Academic Editor: Faiz U. A. Shaikh

The minimum void ratio is a fundamental physical index for evaluating particle properties in soil mechanics, ceramic processing, and concrete mixes. Previous research found that both particle size distribution and particle shape characteristics would affect minimum void ratio, while the current research generally uses a linear model to estimate the minimum void ratio of a binary mixture, ignoring quantitative effect of particle shape on the minimum void ratio. Based on a study of binary mixtures of natural sand from three different origins and iron particles of two different shapes, this paper analyzes the influence factors of the minimum void ratio, and a quadratic nonlinear model is proposed for estimating the minimum void ratio of binary mixture. The model contains only one undetermined coefficient, a, the value of which is correlated to the particle sphericity, particle size, and particle size ratio. A theoretical calculation formula for the coefficient a is proposed to quantitatively analyze the effects of these three factors on the size of the parameters. In the end, the model is used to estimate the minimum void ratios of sand and substitute particles from different producing areas; the average difference between the estimated values and the fitted values is about 2.03%, suggesting that the estimated values of the model fit well with the measured data.

1. Introduction

Granular soil, such as sand and gravel, is a packing of soil particles of different sizes. Due to dispersion of granular materials, the basic properties of particles, such as particle size, particle shape, and friction between particles, all have important impacts on the mechanical properties, resulting in a very complicated macromechanical behavior of granular materials [1–6]. The minimum void ratio represents the densest condition of the soil; it is an important parameter affecting the mechanical behavior of granular soil [7, 8]. Many researchers have obtained the mathematical expressions of the minimum void ratio of sand according to the particle morphology, especially the particle size [9–12] and shape [13–20]. Similar mathematical expressions have been widely used for concrete mixture design to optimize the void ratio of cement, mortar, and concrete [21].

The particle distribution has a significant effect on packing [22, 23]. Cubrinovski and Ishihara [8] examined the influence of fines on the minimum and maximum void ratio by 300 natural sandy soils including clean sands, sands with fines, and sands containing small amount of clay-size particles. Xu et al. [24] measured the minimum void ratio of binary mixed natural sand and binary substitute particles and found that when the fine particle content is about 40%, the minimum void ratio reaches a minimum. Bahari et al. [25] proposed a nonlinear model to estimate the minimum void ratio in sand-silt mixtures with various fines contents.

However, most of these empirical formulas only considered a single variable and ignored the coupling effect of fine particles content and particle shape characteristics on the mixture $e_{\min}$. In fact, for sandy soils, sand shape directly controls the microfabric and hence the shear strength. The influence of sand shape and sorting on mechanical properties of soil depends on fines content, highlighting the complex interaction between particle shape, size, and sorting in their impacting on the mechanical soil behavior [26]. Cubrinovski and Ishihara [8], Santamarina and Cho [14], and Liu et al. [27] showed that a decrease in either sphericity or roundness (increased angularity or plainness) leads to an increase in the dilative response, anisotropic behavior, and peak friction angle and a decrease in rotational movements at particle level. Zhou et al. [28] used discrete element method (DEM) to analyze the effects of particle sphericity on the shearing behavior of soil-structural interface. Chang et al. [29] proposed a linear model which requires only two parameters to predict the minimum void ratios for sand-silt mixtures with different particle sizes. However, there is no specific calculation method for these two shape-related parameters, which limits the applicability of the formula. Xu et al. [24] established a model of the minimum value of the minimum void ratio according to particle sizes and the sphericity of binary mixtures particles based on the experimental data.

This paper attempts to propose a model for predicting the minimum void ratio of binary mixtures based on particle size distribution, regarding the coupling effect of particle shape and particle size.

2. Composition of Binary Mixture

We establish a two-phase diagram for the sand composed of single-size particles as shown in Figure 1(a). The solid volume of the sand particles is denoted by V_{s1}, and the void volume between particles is denoted by V_{v1}. The minimum void ratio of the sand composed of single-size particles is e_1. In order to investigate the relationship between the binary mixture $e_{\min}$ and fine contents, we consider a binary mixture consisting of two different sizes of single-size sand. Figure 1(b) shows the two-phase diagram of mixture in compacted state after adding another particle size of sand (the sand is also composed of single-size particles). The solid volume of the added sand is V_{s2}, and the change of void volume is ΔV_v. The particle sizes of the two components are denoted by d_1 and d_2. The minimum void ratio of the binary mixture is $e_{\min}$.

The mass of the binary mixture is m, and the respective mass fractions of two particles are y_1 and y_2 ($y_1 + y_2 = 1$). The minimum void ratio $e_{\min}$ of mixture can be expressed as

$$e_{\min} = \frac{V_{v1} + nV_v}{V_{s1} + V_{s2}}, \tag{1}$$

$$V_{s1} = \frac{y_1 m}{G_s \rho_w}, \tag{2}$$

$$V_{s2} = \frac{y_2 m}{G_s \rho_w}, \tag{3}$$

$$V_{v1} = e_1 \cdot \frac{y_1 m}{G_s \rho_w}. \tag{4}$$

Substituting V_{s1}, V_{s2}, and V_{v1}, (1) can be rearranged to

$$\Delta V_v = \frac{m}{G_s \rho_w} \cdot e_{\min} - \frac{y_1 m}{G_s \rho_w} \cdot e_1. \tag{5}$$

For a given binary mixture, whose V_{s1}, V_{s2}, and V_{v1} are known, we need the value of ΔV_v to calculate $e_{\min}$ of the mixed particles.

Chang and Meidani [30] assumed that ΔV_v and V_{s2} are linearly correlated and ΔV_v should be related to particle size ratio and morphological properties of sand particles. However, the relationship between ΔV_v and particle morphological characteristics has received little attention.

3. Experimental Study

3.1. Materials. In order to study the influence of particle size ratio, particle shape, and other factors on $e_{\min}$ (i.e., ΔV_v) of binary mixture, we use three types of sands from different origins, which are Dongting Lake Sand (DS), Nanjing River Sand (NS), and Fujian Standard Sand (FS). These natural sand samples are shown in Figure 2, and the particle size distribution curves are shown in Figure 3. For the two morphological characteristics of particle, particle size is usually measured by a standard sieve analysis, and particle shape, including flatness, sphericity, and angularity, is usually analyzed by the binarized image [31, 32]. A large number of representative particles of the three types of natural sand are photographed with a Dino-Lite microscope, and the two-dimensional images are binarized with Photoshop (an example of the microscope image and binarized image is shown in Figure 4). Then the binarized images are analyzed with Image-Pro Plus to get the primary parameters of the particle shapes, such as length L and width B. To further investigate the effects of particle shapes, we choose five different diameter spherical steel balls and three types of cylindrical iron particles as substitute materials which are shown in Figure 5. The five diameters of steel balls ("B" represents steel ball in the following) are 1 mm, 2 mm, 3 mm, 4 mm, and 5 mm, and the three sizes (diameter × height) of cylindrical iron particles ("C" represents cylindrical iron particles in the following) are 0.8 × 0.6 mm, 1.6 × 1 mm, and 2 × 1.5 mm.

The basic physical indicators of the test materials are shown in Table 1. Referring to Xu et al. [24], the particle sphericity, significantly related to the minimum void ratio of binary mixture, is selected as the particle shape description parameter.

3.2. Method. To measure the minimum void ratio of binary mixture, the usual method is to convert the maximum dry density, which is obtained by vibration hammering test method [34]. The vibration hammering method generally uses two kinds of compaction mould (250 ml and 1000 ml). The two compaction buckets have the same height of 18 cm, with corresponding inner diameters of 5 cm and 10 cm. Comparing pretests, we find that although the hammering of compaction barrels with a smaller inner diameter makes the natural sand particles more easily crushed, the compaction work generated is more concentrated, which makes the steel balls and cylindrical iron particles more compact. Therefore, experiments of natural sand use 1000 ml compaction bucket, while experiments of spherical steel balls and cylindrical iron particles use 250 ml bucket.

The first step is to measure the minimum void ratios e_1 of particles in each obtained particle size range of natural sands and substitute materials. The next step is to measure the minimum void ratios $e_{\min}$ of binary mixtures. Then, the corresponding ΔV_v can be obtained.

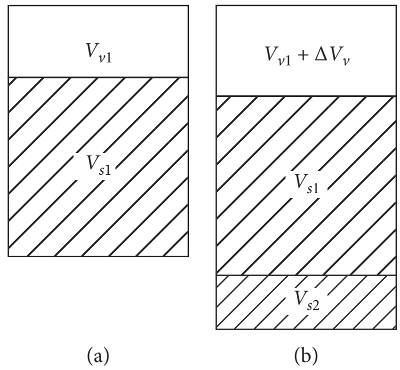

Figure 1: Phase diagram: (a) single-grain sand; (b) binary mixture.

Figure 2: Samples of natural sand: (a) DS; (b) NS; (c) FS.

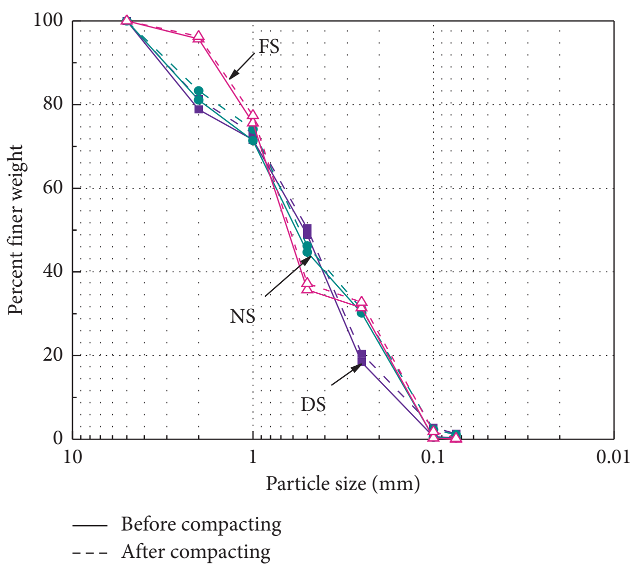

Figure 3: Particle size distribution curves of three types of natural sand.

3.2.1. Minimum Void Ratio e_1 of Each Particle Group. We classify three types of natural sand (i.e., DS, NS, and FS) into five particle groups: 0.1 to 0.25 mm, 0.25 to 0.5 mm, 0.5 to 1 mm, 1 to 2 mm, and 2 to 5 mm particle groups. Among them, the number of particles of 2 to 5 mm in FS is very small, which is difficult to obtain.

We categorize three types of natural sand (i.e., DS, NS, and FS) into five particle groups: 0.1 to 0.25 mm, 0.25 to 0.5 mm, 0.5 to 1 mm, 1 to 2 mm, and 2 to 5 mm. Among them, the content of the particles of 2 to 5 mm in FS is very small, making it hard to obtain, so the FS lacks the particle group of 2 to 5 mm. For convenience, the average value of the upper and lower boundary particle sizes of each particle group is used to represent the particle size of the particle group, which is 0.175, 0.375, 0.75, 1.5, and 3.5 mm. These particle groups can be seen as single-sized particle groups composed of particles with corresponding average particle size. We measure the minimum void ratio e_1 of each particle group, spherical steel balls, and cylindrical iron particles.

3.2.2. Minimum Void Ratio e_{min} of Binary Mixtures. First, we mix two different particle groups from the same area with different mass ratios (i.e., different ratios of y_1 and y_2) to form a binary mixture, and measure the corresponding minimum void ratio e_{min} of binary mixture. Then the corresponding void volume change ΔV_v can be calculated from (5), and the relations between ΔV_v and particle properties parameters can be estimated.

4. Results and Discussion

4.1. Experimental Results and Analysis for Binary Mixture

4.1.1. Variation of Minimum Void Ratios (e_{min}). The experimental values of minimum void ratio are plotted against particle content in Figure 7. It shows that the curves are

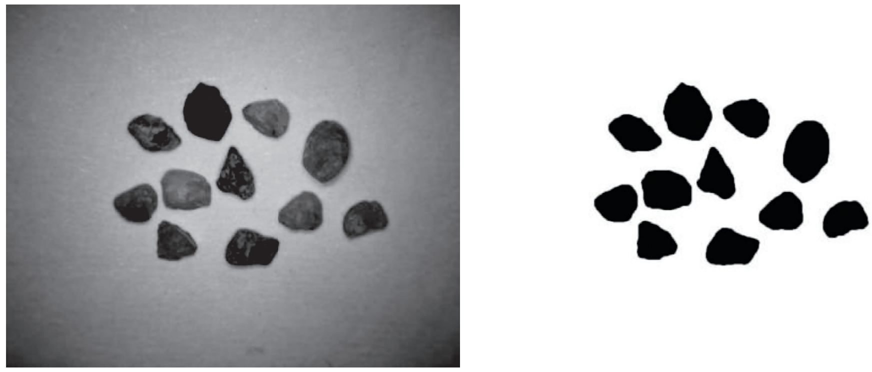

(a) (b)

Figure 4: Microscope image and binarized image.

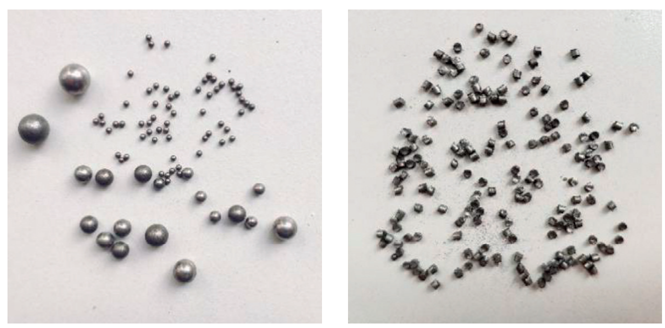

(a) (b)

Figure 5: Samples of synthetic materials: (a) *B*; (b) *C*.

Table 1: Some physical properties of the materials tested.

Sand	d_{10} (mm)	d_{30} (mm)	d_{60} (mm)	C_u	C_c	G_s	S
NS	0.13	0.23	0.76	5.85	0.54	2.64	0.5632
DS	0.16	0.32	0.71	4.44	0.90	2.64	0.5687
FS	0.13	0.22	0.80	6.15	0.47	2.62	0.5894
B	—	—	—	—	—	7.97	1.000
C	—	—	—	—	—	7.45	0.6260

Note. $C_u = d_{60}/d_{10}$; $C_c = (d_{30})^2/(d_{60} * d_{10})$. S is the sphericity of the particles, describing how close the particle comes to the shape of a sphere. The value of S is given by $S = R_i/R_c$ [33], where R_i is the maximum radius of the tangential circle of the particle and R_c is the minimum radius of the circumferential circle of the particle, as shown in Figure 6.

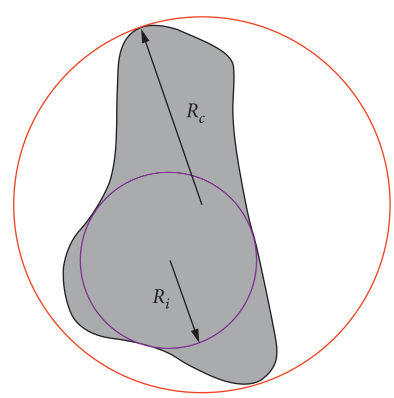

Figure 6: Geometric parameters used in the definition of sphericity (S).

V-shaped, suggesting that when the fine particle content increases, the minimum void ratio of the binary mixture decreases first and then increases. As observed from the curves of different particle size differences, the larger the difference in particle size is, the more obvious the V-shape is. For a given binary mixture, there is an optimal ratio that minimizes the minimum void ratio of the binary mixture. The experimental results show that the optimal fine particle content of the binary mixture is between 30% and 40%, which is in good agreement with previous seminal works including Assadi-Langroudi [26], Thevanayagam and Mohan [35], Xenaki and Athanasopoulos [36], and Yang and Wei [37]. Assadi-Langroudi found that when the silt content is 37%, the minimum void ratio reaches a lower limit of 0.38.

4.1.2. Effect of Particle Size Ratio on Void Volume Change (ΔV_v). Figure 8 shows the variation of the void volume change of the binary mixture versus the solid volume of fine particles added. It is obvious that the particle size ratio has a great effect on the relationship curve of $\Delta V_v - V_{s2}$. For different materials, it tends to be a straight line when the particle size ratio is close to 1, while the nonlinear trend of the curve becomes more obvious when the particle size ratio is close to 0. The reason should be the embedding and filling effect as shown in Figure 9. The particles are simply stacked up, instead of mutual-filling when the difference of particle sizes is small enough, while the fine particles would fill the void between the coarse particles when the difference between d_1 and d_2 is large enough. In the latter case, the ΔV_v gradually decreases until the void is completely filled, and then ΔV_v increases with the fine particles.

In Figure 8, it also can be seen that when the binary mixture has the same fine particle content, the smaller the d/D, the smaller the ΔV_v and the smaller the corresponding $e_{\min}$. This trend is consistent with the findings by McGeary [38], who pointed out that when the difference in particle size of the two particles increases (or d/D decreases), the packing density increases (or the void ratio decreases).

4.1.3. Effect of Particle Shape on Void Volume Change (ΔV_v). To study the influences of particle shapes on the void volume change, we compare curves of $\Delta V_v - V_{s2}$ for different sand mixtures under the same particle size combination, as shown in Figure 10.

As observed from the curves in Figure 10, even if the particle size combinations are the same, the relationship curves of $\Delta V_v - V_{s2}$ are different. It is noted that the curves of $\Delta V_v - V_{s2}$ under the same particle size combinations from high to low are NS, DS, and FS, whose arrangement order is consistent with that of sphericity. Sphericity proves to be an essential characteristic parameter [24], which directly determines how particles of the mixture contact with each other and in turn affect the particle structure inside the mixture. The test result above further proves that the void volume change of binary mixture is also affected by the shapes of the particles.

4.1.4. Effect of Particle Size of Fine Particles on Void Volume Change (ΔV_v). Comparing the curves of ΔV_v with solid volume of the added sand, we find that even if the binary mixtures are from the same origin and at the same particle size ratio, the curves of ΔV_v-V_{s2} are not completely consistent, as shown in Figure 11. The test result shows that the larger the fine particle size is, the larger the ΔV_v of the binary mixture is, which can be attributed to particle size difference and deviation of particle shapes between large and small particles [39]. These two factors may contribute to the difference in total area of interparticle contact, resulting in a difference in ΔV_v.

4.2. Prediction Model of Minimum Void Ratio of Binary Mixture

4.2.1. Preliminary Model for Estimating Minimum Void Ratio of Binary Mixture. Here, we aim to build a model for predicting minimum void ratio or the void volume change as a function of fines content. For convenience, the relationship between ΔV_v and V_{s2} in the previous section is converted to the relationship of $(\Delta V_v)/V$ and y_2. As described in the previous section, the particle size ratio, sphericity, and fine particle size have a significant effect on the change in void volume. Since natural sand mixtures deviate much more in particle shapes and particle distribution, it is not realistic to have a universal equation for void volume change. It is more practical to model the particle behavior with different parameters.

In Figure 12, the fitting curves generated by JMP 13 PRO software show a significant quadratic relationship between $(\Delta V_v)/V$ and y_2 in natural binary mixtures and iron particle mixtures, as shown in

$$\frac{\Delta V_v}{V} = a y_2^2 + b y_2 + c, \quad y_S \in [0,1], \tag{6}$$

where coefficients a, b, and c are material coefficients corresponding to different binary mixtures. Table 2 presents different values of the coefficients a, b, and c for various types of binary mixture based on particle shape and particle size effect.

The coefficients of determination (R^2) of the regression in Table 2 are very high for all materials, which means that most variations in dependent variable $\Delta V_v/V$ can be explained by independent variable y_2 in (6).

Applying (6) to (1) gives

$$e_{\min} = \frac{V_{v1} + V \cdot \left(a y_2^2 + b y_2 + c\right)}{V_{s1} + V_{s2}}. \tag{7}$$

The total volume of the binary mixture in the densest state is

$$V = V_s + V_v = V_s + e_{\min} \cdot V_s = \frac{m}{G_s \cdot \rho_w} + e_{\min} \cdot \frac{m}{G_s \cdot \rho_w}. \tag{8}$$

Applying (2), (3), (4), and (8) to (7) gives the estimated equation of $e_{\min}$:

$$e_{\min} = \frac{e_1 y_1 + a y_2^2 + b y_2 + c}{1 - a y_2^2 - b y_2 - c}. \tag{9}$$

Equation (8) gives a preliminary equation to estimate the minimum void ratio of a binary mixture. However, the three coefficients a, b, and c are different when the type of mixtures changes, making the equation inconvenient for subsequent study. To avoid this inconvenience and to make the estimation formula more applicable, the relationship and values of coefficients a, b, and c in the formula are further explored based on limiting states.

It has been pointed out in the previous section that (6) applies to $y_2 \in [0,1]$.

(1) Limiting State One. When $y_2 = 0$, the mixture is completely composed of coarse particles (Figure 13(a)).

The corresponding $\Delta V_v = 0$.

Substituting $\Delta V_v = 0$ into (6) gives

$$c = 0. \tag{10}$$

According to Table 2, based on the regression results of the relationship curve between $\Delta V_v/V$ and y_2, regardless of whether it is a natural sand mixture or a substitute particle mixture, the coefficient c is an order of magnitude smaller than a and b, where c is close to 0. In particular, we consider particles with a single-grain particle size as a special case of binary mixtures. It is found that the coefficient c for particles with a single-grain particle size is 0, which suggests that the coefficient c is an experimental error.

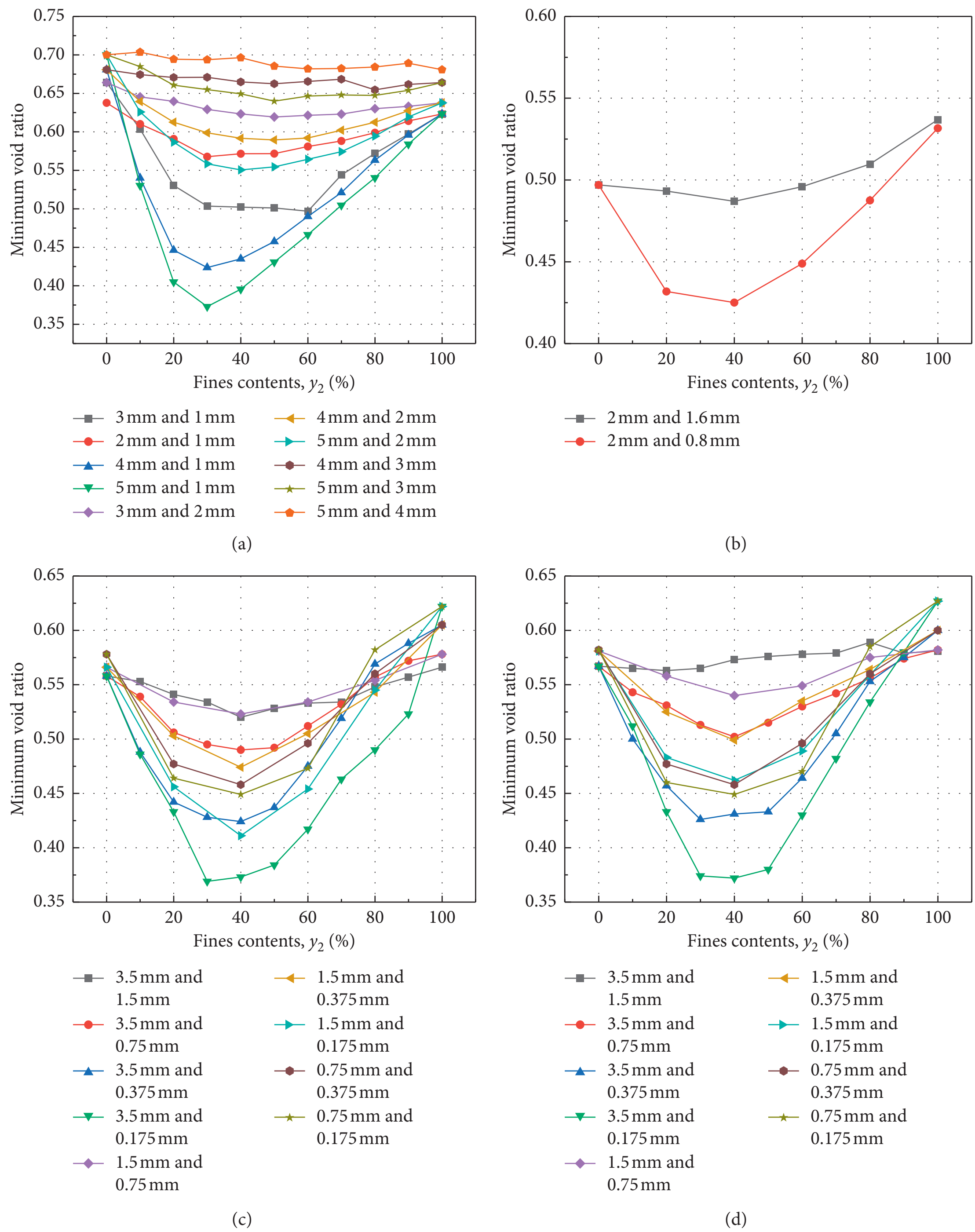

Figure 7: Continued.

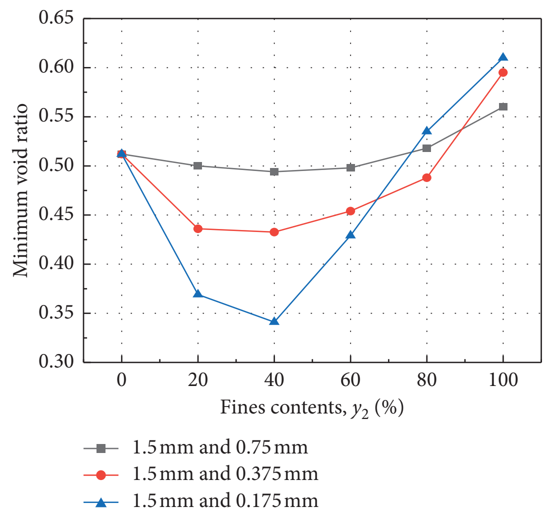

(e)

Figure 7: Measured minimum void ratios versus fines content: (a) *B*; (b) *C*; (c) DS; (d) NS; (e) FS.

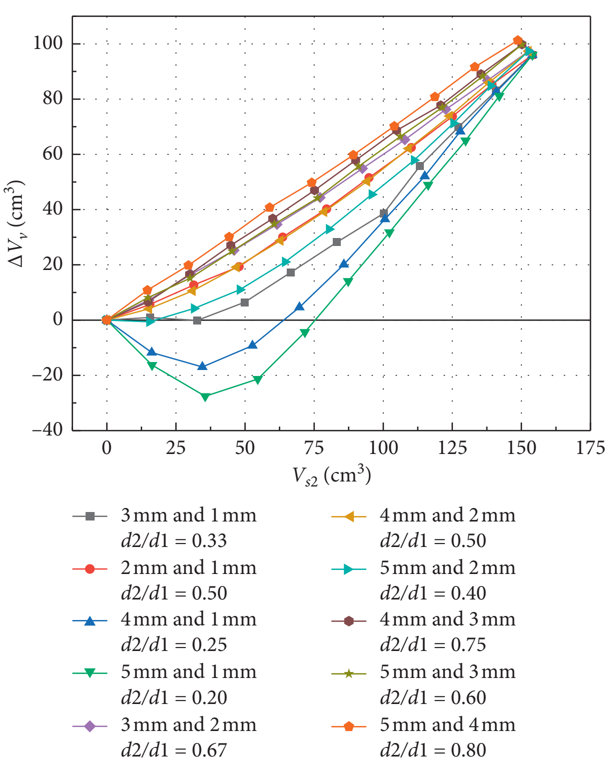

(a)

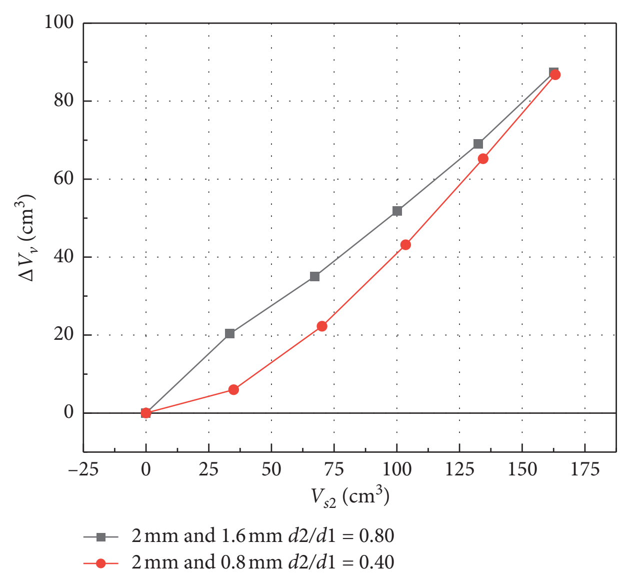

(b)

Figure 8: Continued.

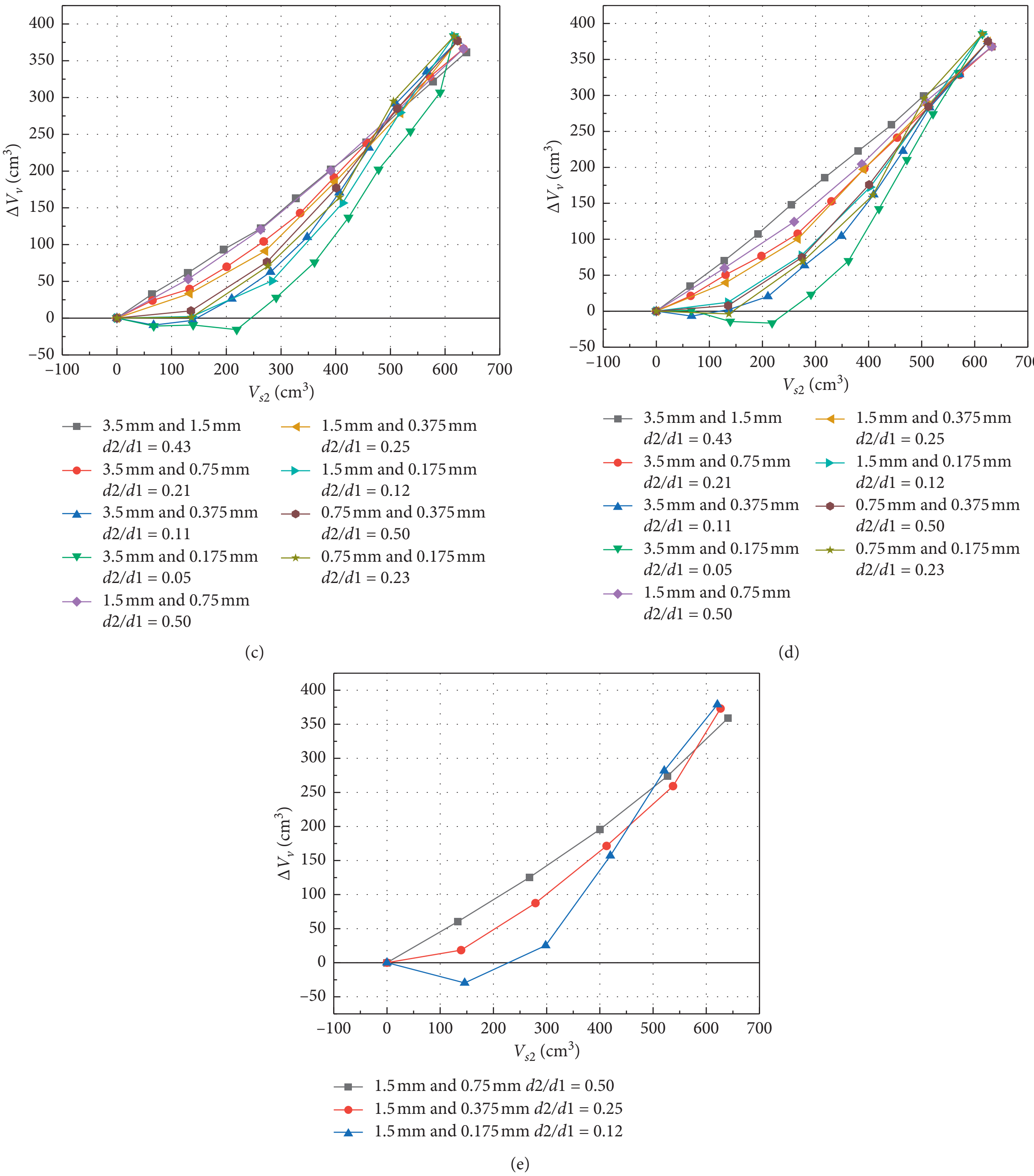

Figure 8: Variation of Void volume change with solid volume of fine particles: (a) B; (b) C; (c) DS; (d) NS; (e) FS.

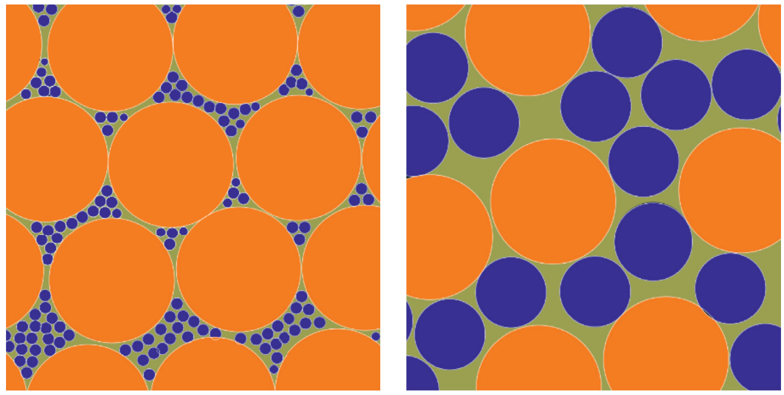

Figure 9: Stacking and filling effect: (a) filling effect; (b) embedding effect.

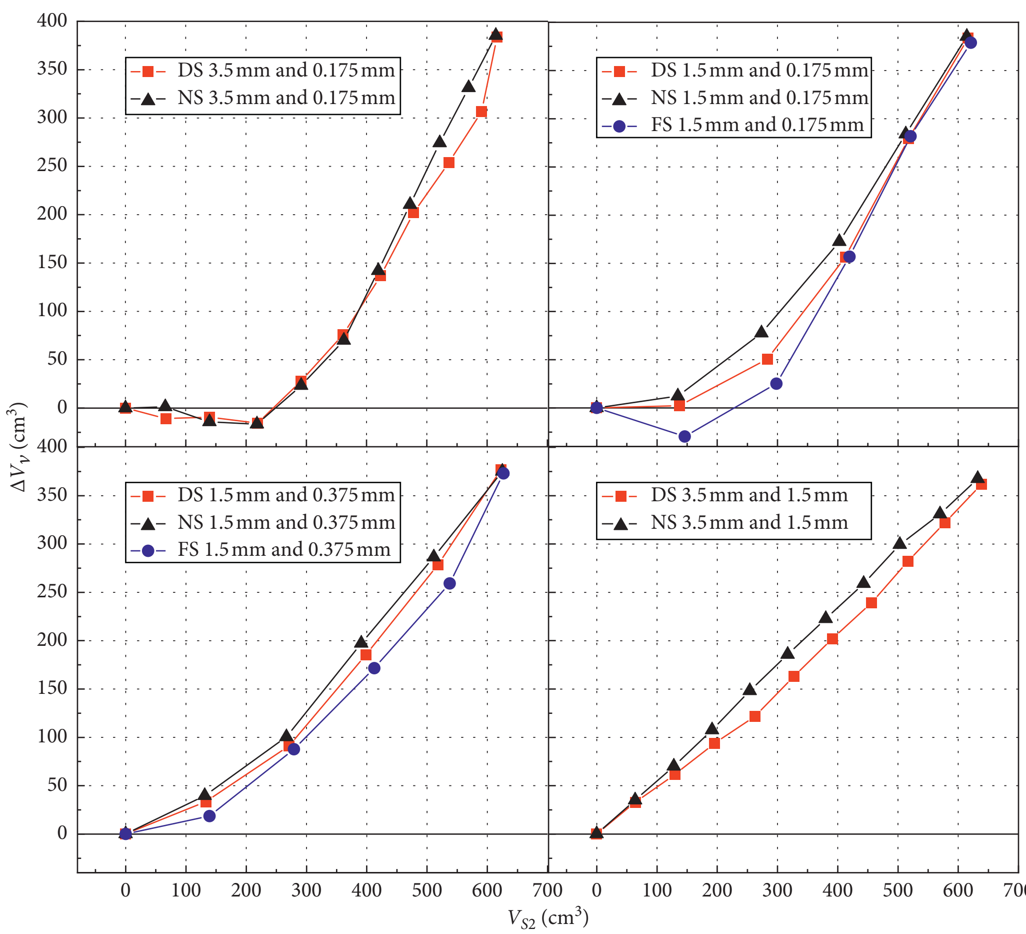

Figure 10: Comparison of $\Delta V_v - V_{s2}$ curves under the same particle size combination.

(2) Limiting State Two. When $y_2 = 1$, the mixture is completely composed of fine particles (Figure 13(b)).

The corresponding $\Delta V_v = V_{v2}$.

$$\frac{\Delta V_v}{V} = \frac{V_{v2}}{V_{v2} + V_{s2}} = \frac{e_2 \cdot V_{s2}}{e_2 \cdot V_{s2} + V_{s2}} = \frac{e_2}{e_2 + 1}. \tag{11}$$

Substituting $c = 0$, $y_2 = 1$, and (10) in (6) gives

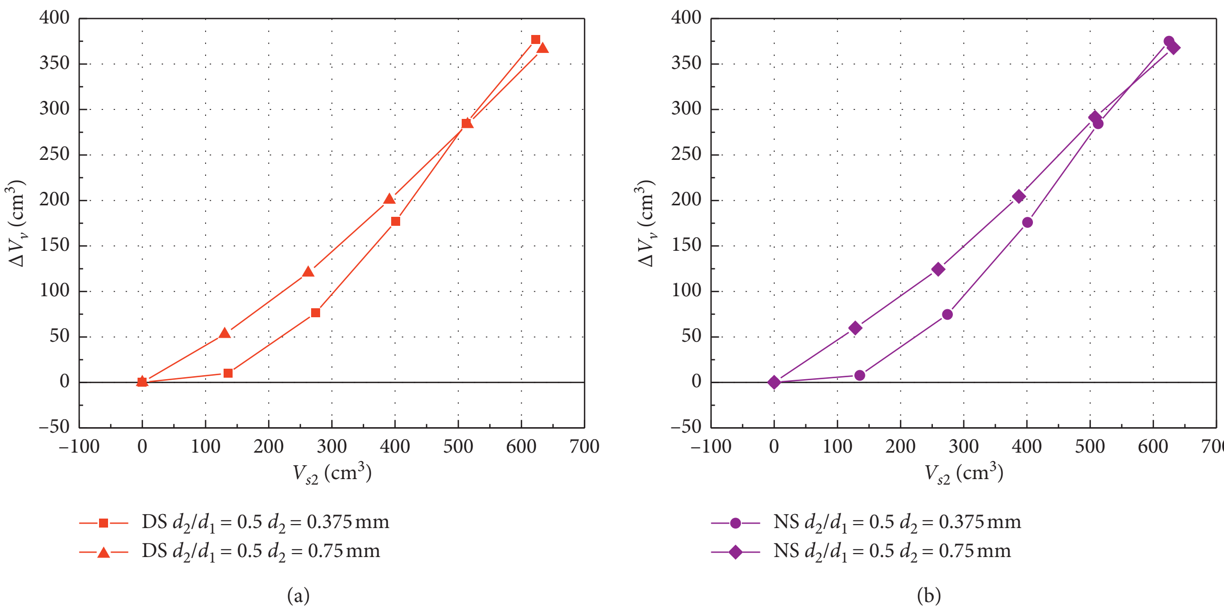

Figure 11: Comparison of ΔV_v-V_{s2} curves under the same particle size ratio.

$$a + b = \frac{e_2}{e_2 + 1}. \tag{12}$$

According to Figure 14, based on the regression result of (6)—the equation of $\Delta V_v/V$ and y_2—the measured sum of a and b is very close to $e_2/(e_2+1)$. Thus, coefficient b can be replaced by $((e_2)/(e_2+1)) - a$.

After the above limiting state analysis, (9) can be rearranged to (13)

$$e_{\min} = \frac{e_1 y_1 + a y_2^2 + (((e_2)/(e_2+1)) - a) y_2}{1 - a y_2^2 - (((e_2)/(e_2+1)) - a) y_2}. \tag{13}$$

4.2.2. Prediction Model of Coefficient **a**. Equation (13) is an equation of the minimum void ratio of the binary mixture as a function of fines content, where coefficient a is the only unknown coefficient, defined as the coefficient of influence of the pore volume of the binary mixture. The value of coefficient a will be further analyzed below.

Figure 15 summarizes the relationship between the void volume influence coefficient a and the particle size ratio d_2/d_1 of different types of binary mixtures. Figure 15 suggests that, for various binary mixtures, coefficient a decreases as the particle size ratio increases. For mixtures with a particle size ratio of 1 (i.e., single-size sand), coefficient a equals 0.

In addition, for three kinds of natural sand, the coefficient a decreases as the particle size increases even if the particle size ratio is the same, whereas, for spherical steel balls, regardless of particle size, the corresponding coefficient is the same as long as the particle size ratio is of almost equal value. Therefore, for natural irregular particles, the dispersion of particle distribution and particle shape must be considered in modeling.

Figure 16 compares the curves between coefficient a and the particle size ratio d_2/d_1 for different binary mixtures under the same particle size combination. It is noted that, under the same particle size combination, the natural sand is arranged by FS, DS, and NS according to a coefficient from large to small. It can be seen that the order of arrangement is the same as the change of sphericity. Coefficient a increases as the sphericity of the binary mixture increases.

Since the value of coefficient a is significantly related to the particle size ratio d_2/d_1, the fine particle size d_2, and the sphericity S for natural sand, the regression equation based on coefficient a in Table 2 is given as follows:

$$a = 0.013 * \left(\frac{d_1}{d_2}\right) - 0.195 * d_2 + 0.819 * S - 0.211. \tag{14}$$

However, according to Figure 15, for spherical steel balls, the coefficient is highly related to the particle size ratio, but not to the other two parameters, so we derive the following regression equation:

$$a = 0.152 * \left(\frac{d_1}{d_2}\right) - 0.158. \tag{15}$$

In order to verify the accuracy of the regression equations (14) and (15), the coefficient a values of the different mixtures estimated with (14) and (15) are compared with the fitted values in Table 2, as shown in Figure 17. It can be found that the difference between the estimated value and the fitted value is small, with the average discrepancy being approximately 2.5%.

4.2.3. Prediction Equation of Minimum Void Ratio. Combining (13) and (14) makes it possible to estimate $e_{\min}$ of the natural sand binary mixture under each particle size combination and particle proportion.

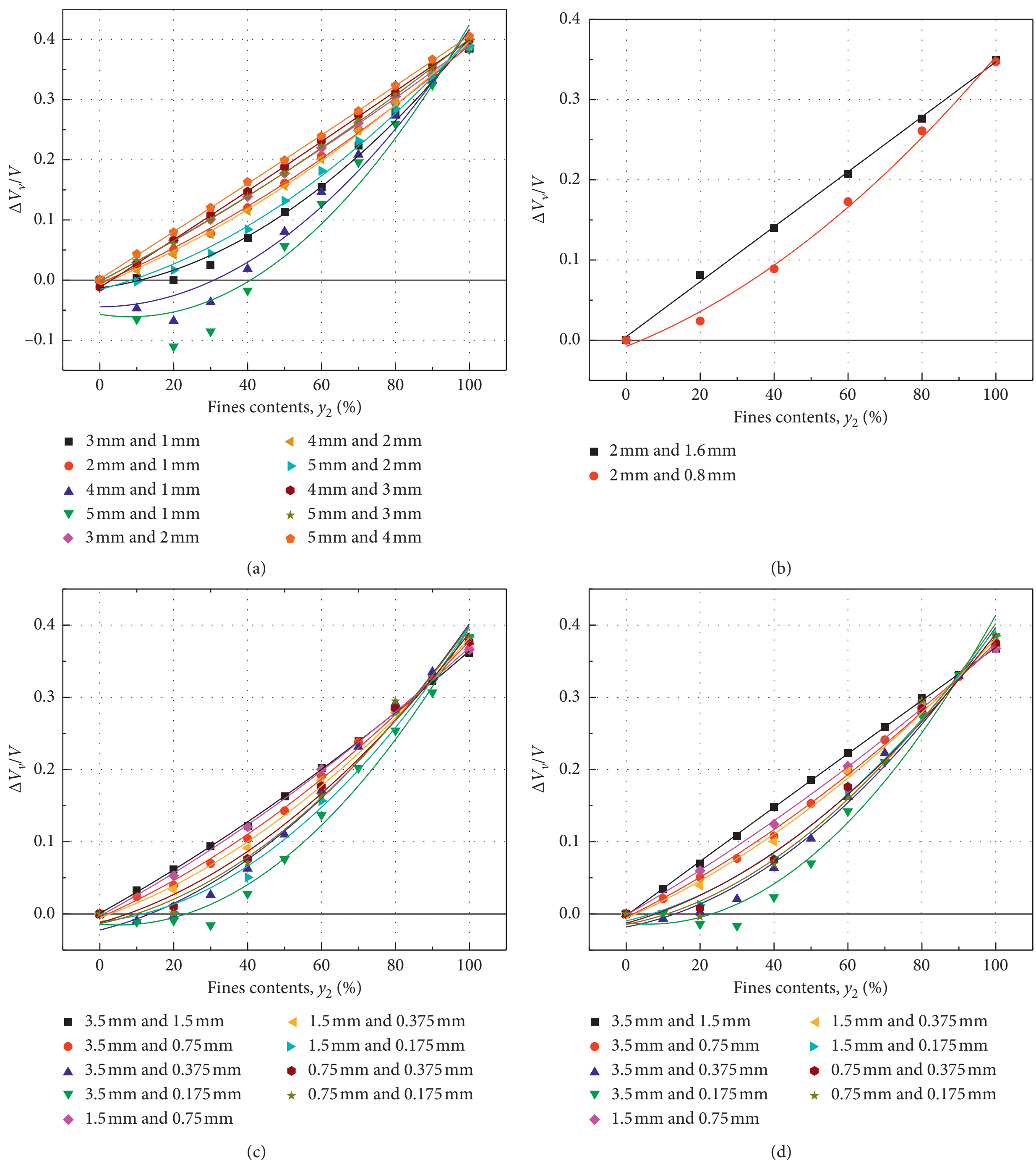

FIGURE 12: Continued.

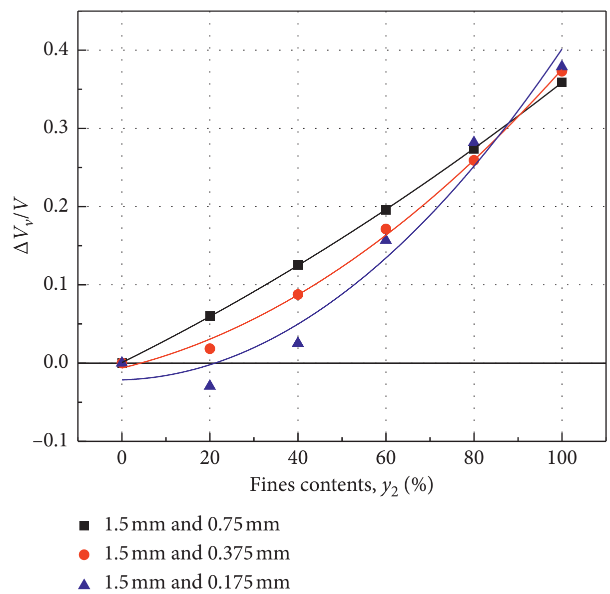

(e)

FIGURE 12: Fitting curves of $\Delta V_v/V$ and y_2 for various types of binary mixture: (a) *B*; (b) *C*; (c) DS; (d) NS; (e) FS.

TABLE 2: The fitting results of the relationship curve between $\Delta V_v/V$ and y_2.

Equation Particle	Particle size combination (mm)	$(\Delta V_v/V) = ay_2^2 + by_2 + c$ *a*	*b*	*c*	R^2
SB	2-1	0.1264378	0.2696234	−0.005658	0.998671
SB	3-1	0.3337977	0.0802365	−0.012969	0.992375
SB	4-1	0.4597071	0.0014724	−0.044485	0.968989
SB	5-1	0.5774216	−0.0959275	−0.056986	0.951515
SB	3-2	0.0649727	0.3293016	−0.002488	0.999827
SB	4-2	0.1520245	0.2521251	−0.007970	0.998662
SB	5-2	0.2562652	0.1611679	−0.015718	0.995338
SB	4-3	0.0172446	0.3939407	−0.012418	0.999878
SB	5-3	0.0836125	0.3196165	−0.002109	0.99968
SB	5-4	0.0138963	0.3904136	0.001639	0.999833
DS	3.5-1.5	0.0776366	0.2856906	0.000768	0.999592
DS	3.5-0.75	0.1574867	0.2254102	−0.005103	0.996808
DS	3.5-0.375	0.2999622	0.1242011	−0.022362	0.986161
DS	3.5-0.175	0.4574682	−0.0463245	−0.014161	0.988263
DS	1.5-0.75	0.09422	0.2777333	−0.002779	0.999374
DS	1.5-0.375	0.2087487	0.1789838	−0.005167	0.997483
DS	1.5-0.175	0.3603429	0.0475395	−0.010514	0.990399
DS	0.75-0.375	0.2575182	0.1439691	−0.012242	0.990746
DS	0.75-0.175	0.3047703	0.1083967	−0.013598	0.98741
NS	3.5-1.5	−0.0060418	0.377529	−0.002553	0.999727
NS	3.5-0.75	0.1274844	0.2534506	−0.005039	0.998116
NS	3.5-0.375	0.3196639	0.0952239	−0.018099	0.989217
NS	3.5-0.175	0.4853658	−0.0593874	−0.012324	0.981702
NS	1.5-0.75	0.0775183	0.29591	−0.001764	0.999125
NS	1.5-0.375	0.1604153	0.2270598	−0.005972	0.99655
NS	1.5-0.175	0.2815766	0.1236601	−0.009821	0.994165
NS	0.75-0.375	0.2592462	0.1416453	−0.012941	0.989718
NS	0.75-0.175	0.3186972	0.0980947	−0.014676	0.986183
FS	1.5-0.75	0.0993705	0.2586448	0.000537	0.99998
FS	1.5-0.375	0.2464325	0.1351866	−0.006370	0.997581
FS	1.5-0.175	0.407979	0.0149573	−0.021548	0.972988
C	2-1.6	0.0483006	0.2787614	0.022205	0.998634
C	2-0.8	0.1804557	0.1808277	−0.007570	0.99597

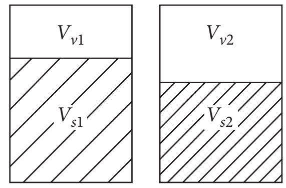

(a) (b)

Figure 13: (a) $y_2 = 0$, only coarse particle. (b) $y_2 = 1$, only fine particle.

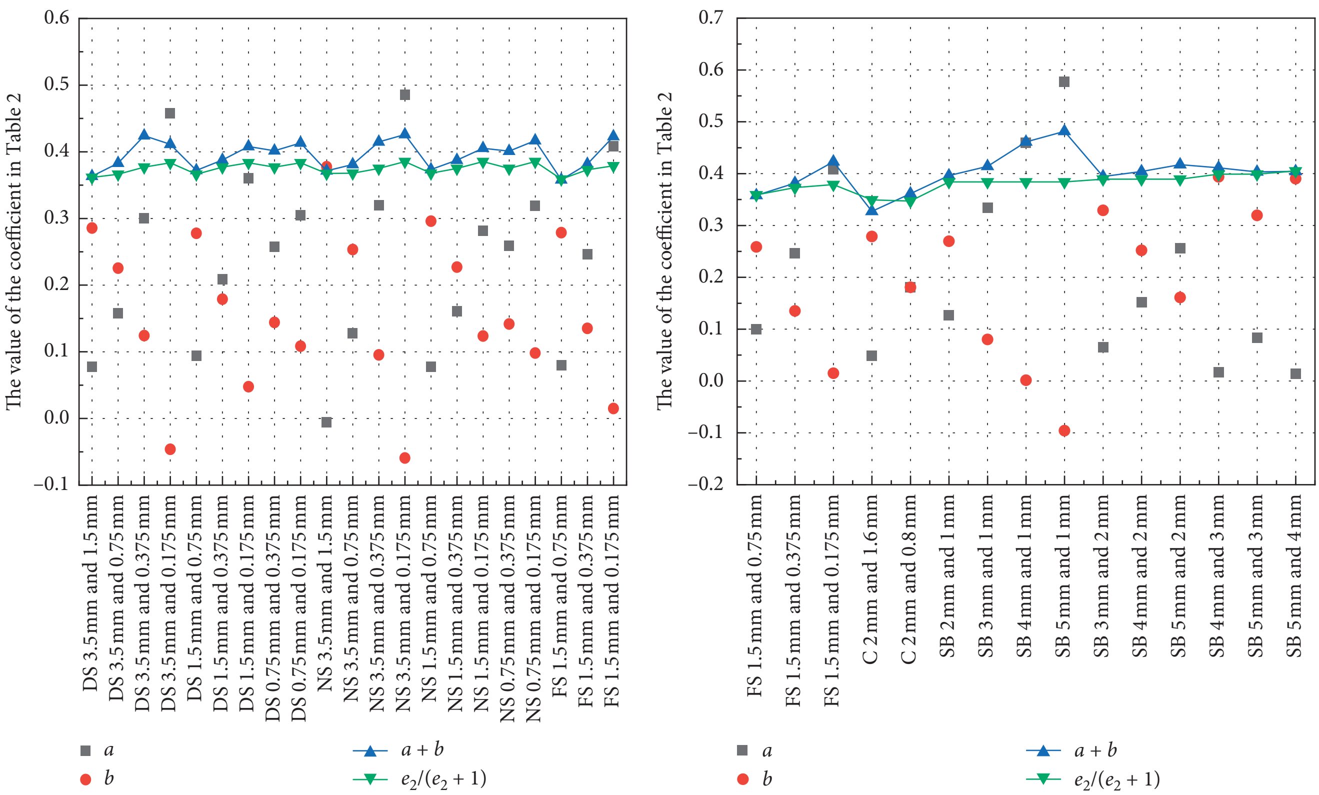

(a) (b)

Figure 14: Comparison chart of $(a + b)$ and $e_2/(e_2 + 1)$.

$$\begin{cases} ne_{\min} = \dfrac{e_1 y_1 + a y_2^2 + (((e_2)/(e_2+1)) - a) y_2}{1 - a y_2^2 - (((e_2)/(e_2+1)) - a) y_2}, \\[2ex] na = 0.013 * \left(\dfrac{d_1}{d_2}\right) - 0.195 * d_2 + 0.819 * S - 0.211. \end{cases} \tag{16}$$

For a binary mixture of spherical steel balls, the prediction formula for the minimum void ratio can be expressed as

$$\begin{cases} ne_{\min} = \dfrac{e_1 y_1 + a y_2^2 + (((e_2)/(e_2+1)) - a) y_2}{1 - a y_2^2 - (((e_2)/(e_2+1)) - a) y_2}, \\[2ex] na = 0.152 * \left(\dfrac{d_1}{d_2}\right) - 0.158. \end{cases} \tag{17}$$

In order to verify the accuracy of the joint equations (16) and (17), $e_{\min}$ values of different mixtures estimated by (16) and (17) are compared with the measured $e_{\min}$ value of each corresponding binary mixture in the experiment, as shown

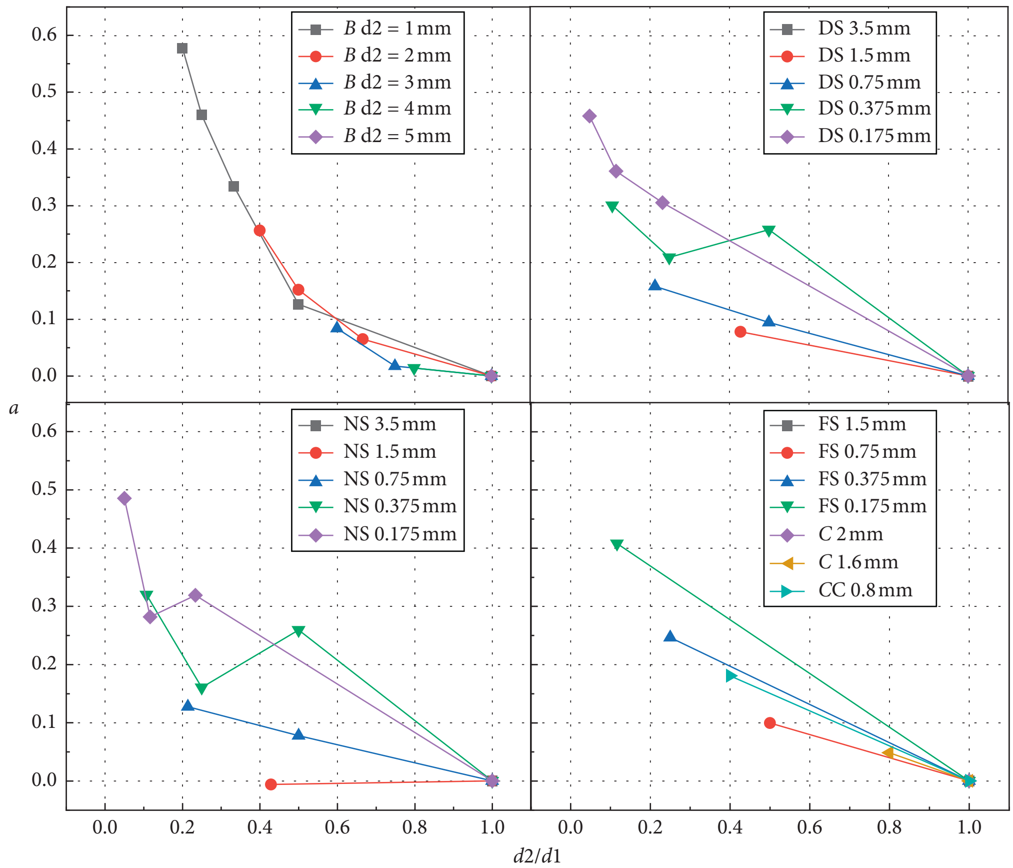

FIGURE 15: Curves of a and d_2/d_1 for the binary mixtures.

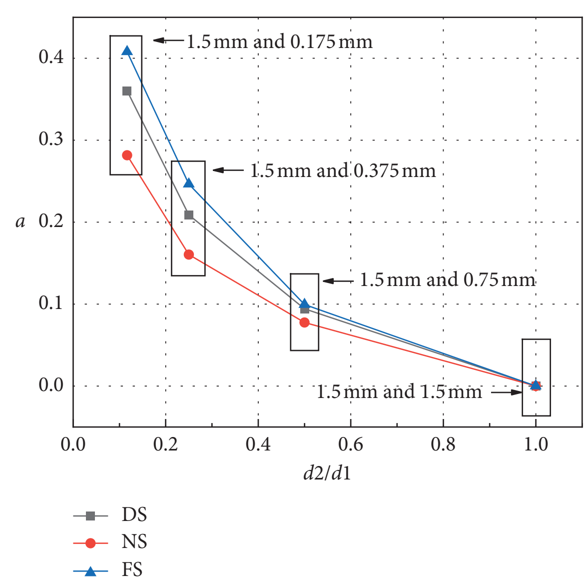

FIGURE 16: Curves of a and d_2/d_1 under the same particle size combination.

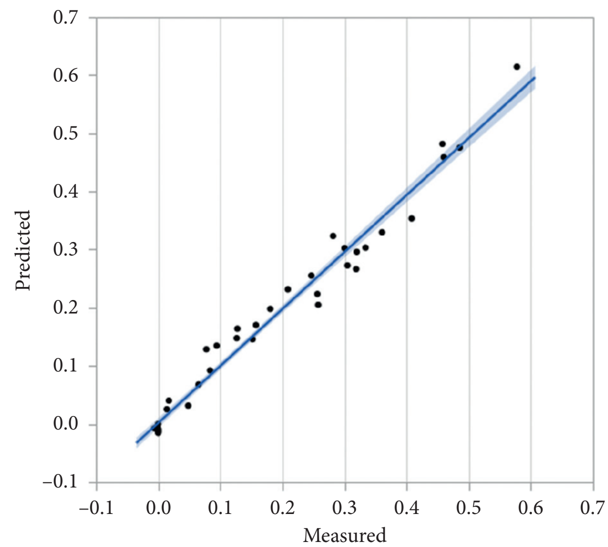

Figure 17: Comparison between coefficient a measured and estimated by (14) and (15).

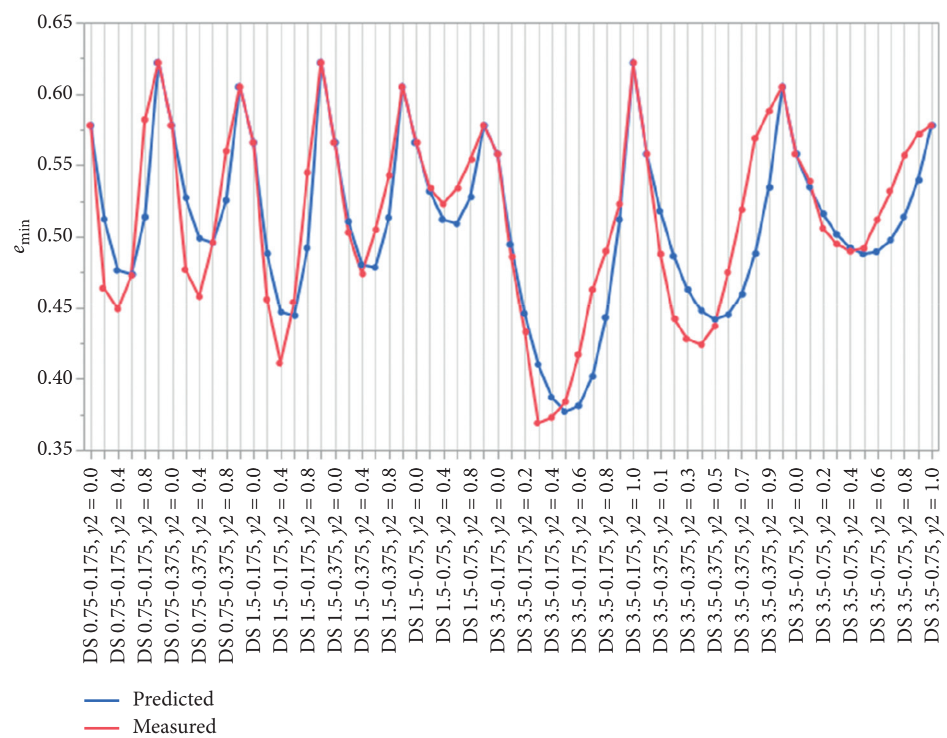

(a)

Figure 18: Continued.

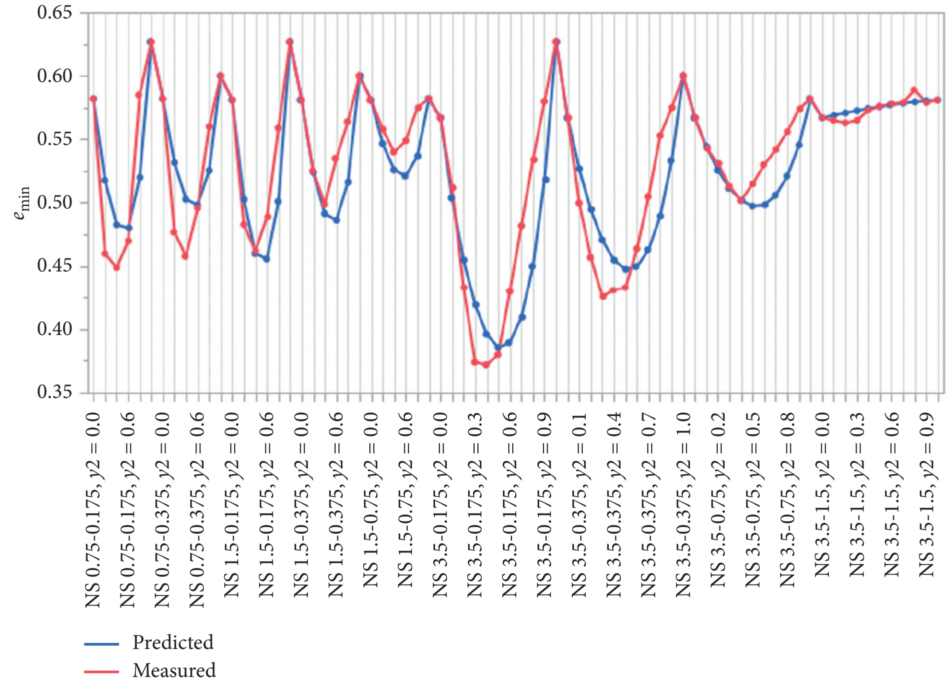

(b)

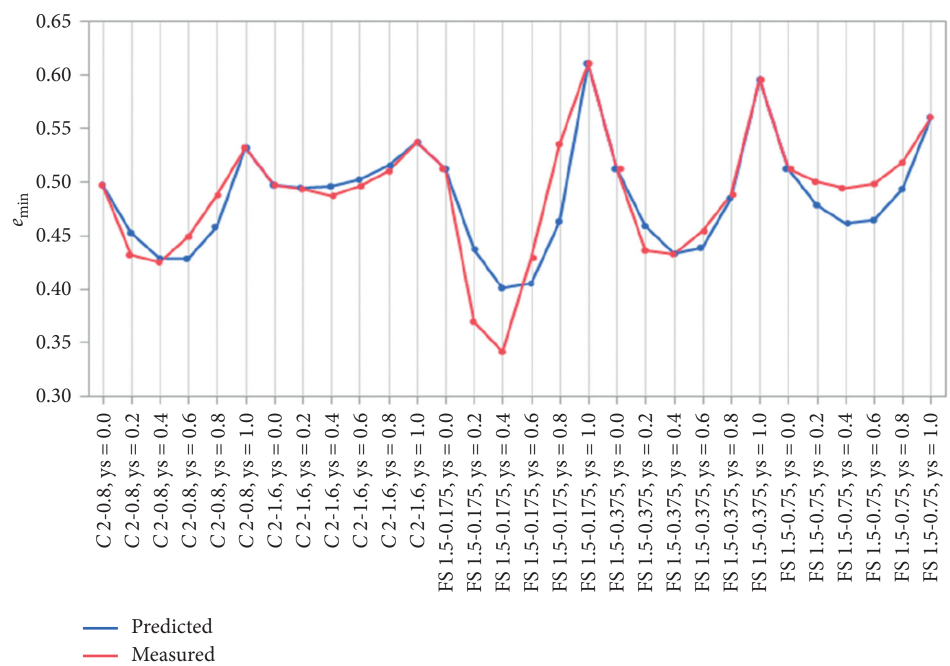

(c)

Figure 18: Continued.

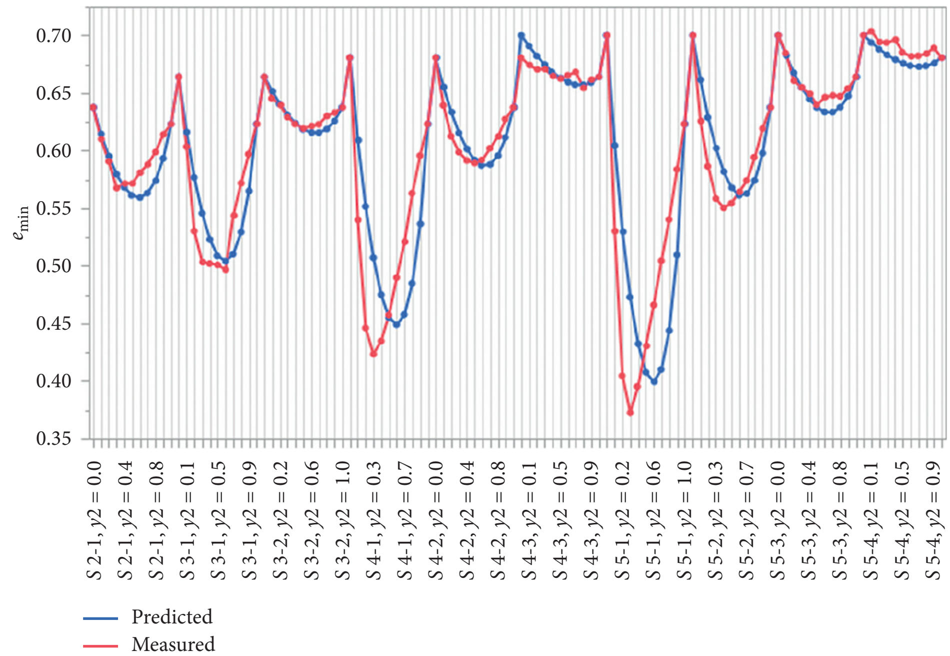

(d)

FIGURE 18: Comparison between the predicted and measured $e_{\min}$.

in Figure 18. The average difference between the estimated and measured e_{min} is about 2.03%, suggesting that the regression equations (16) and (17) have high estimation accuracy. Therefore, it is feasible to obtain coefficient a by the above joint equations to estimate $e_{\min}$.

However, the type of sand used is less and the shape is close. In order to determine the precise numerical relationships between the pore volume influence coefficient a and d_2/d_1, d_2, and S, more natural sand with different shape parameters needs to be introduced to the experiment.

5. Conclusion

Based on a study of binary mixtures of natural sand from three different origins and iron particles of two different shapes, this paper analyzes the influence factors of the minimum void ratio. It is found that when the $e_{\min}$ value of the binary mixture reaches the minimum, the percentage of corresponding fine content is approximately 30–40%. For binary mixtures, the particle size ratio, the size of the fine particles, and the shape of the particles will affect the value of $e_{\min}$. In this paper, sphericity is used to quantify the effect of particle shape. The decrease of the particle size ratio d/D, the increase of the sphericity S, and the decrease of the fine particle size will all lead to the decrease of the minimum void ratio of the binary mixture.

Based on the experimental data, a new quadratic polynomial model is developed to predict $e_{\min}$ value as a function of fines content for various binary sand mixtures. This prediction model requires only one undetermined coefficient, a. Using the nonlinear model, the minimum void ratios of mixtures (286 types of various binary mixtures) are predicted. The average discrepancy between predicted and measured void ratios is about 2.03%. Therefore, quadratic polynomial prediction is reasonable and feasible.

However, the particle shape parameters of the sand used in practice are relatively inadequate, and in the experiment, there is a lack of alternative materials with the same particle size as sand. Thus, this type of investigation will be conducted in future work to improve the accuracy of prediction.

Data Availability

The data used to support the findings of this study are available from the corresponding author upon request.

Additional Points

Highlights. Particle shape, particle size ratio, and fine particle size affect the minimum void ratio of binary particle mixtures. The effect of particle sphericity on minimum porosity of binary mixture is quantitatively analyzed. A model for predicting the minimum void ratio based on particle size distribution is proposed. The model considers the coupling effect of particle size and particle shape.

Conflicts of Interest

The authors declare that there are no conflicts of interest.

Acknowledgments

The authors would like to acknowledge the financial support from the National Natural Science Foundation Committee of China (no. 51278446).

References

[1] J. Yang, "Non-uniqueness of flow liquefaction line for loose sand," *Géotechnique*, vol. 52, no. 10, pp. 757–760, 2002.

[2] J. Yang and X. S. Li, "State-dependent strength of sands from the perspective of unified modeling," *Journal of Geotechnical and Geoenvironmental Engineering*, vol. 130, no. 2, pp. 186–198, 2004.

[3] Z. Y. Cai and X. S. Li, "Deformation characteristics and critical state of sand," *Chinese Journal of Geotechnical Engineering*, vol. 26, no. 5, pp. 697–701, 2004.

[4] Y. Xiao and L. Long, "Effect of particle shape on stress-dilatancy responses of medium-dense sands," *Journal of Geotechnical and Geoenvironmental Engineering*, vol. 145, no. 2, Article ID 04018105, 2019.

[5] J. Yang and X. D. Luo, "Exploring the relationship between critical state and particle shape for granular materials," *Journal of the Mechanics and Physics of Solids*, vol. 84, pp. 196–213, 2015.

[6] G. Sezer A and A. B. Ktepe, "Effect of particle shape on density and permeability of sands," *Proceedings of the Institution of Civil Engineers - Geotechnical Engineering*, vol. 163, no. 6, pp. 307–320, 2010.

[7] E. Seling and R. Ladd, *Evaluation of Relative Density Measurements and Applications*, ASTM International, West Conshohocken, PA, USA, 1973.

[8] M. Cubrinovski and K. Ishihara, "Maximum and minimum void ratio characteristics of sands," *Soils and Foundations*, vol. 42, no. 6, pp. 65–78, 2002.

[9] K. Miura, K. Maeda, M. Furukawa, and S. Toki, "Physical characteristics of sands with different primary properties," *Soils and Foundations*, vol. 37, no. 3, pp. 53–64, 1997.

[10] S. K. Rout, *Prediction of Relative Density of Sand with Particular Reference to Compaction Energy*, National Institute of Technology, Rourkela, India, 2009.

[11] C. Patra, N. Sivakugan, B. Das, and S. Rout, "Correlations for relative density of clean sand with median grain size and compaction energy," *International Journal of Geotechnical Engineering*, vol. 4, no. 2, pp. 195–203, 2010.

[12] J. R. Chen and F. H. Kulhawy, "Characteristics and intercorrelations of index properties for cohesionless gravelly soils," in *Proceedings of the GeoCongress 2014: Geo-Characterization and Modeling for Sustainability*, pp. 1–13, Atlanta, GA, USA, February 2014.

[13] S. Shimobe and N. Moroto, "A new classification chart for sand liquefaction," in *Proceedings of 1st International Conference Earthquake Geotechnical Engineering*, Ishihara, Ed., pp. 315–320, 1995.

[14] J. C. Santamarina and G. C. Cho, "Soil behaviour: the role of particle shape," in *Advances in Geotechnical Engineering: Proceedings of the Skempton Conference*, R. J. Jardine, D. M. Potts, and K. G. Higgins, Eds., vol. 1, pp. 604–617, Thomas Telford, London, UK, 2004.

[15] G.-C. Cho, J. Dodds, and J. C. Santamarina, "Particle shape effects on packing density, stiffness, and strength: natural and crushed sands," *Journal of Geotechnical and Geoenvironmental Engineering*, vol. 132, no. 5, pp. 591–602, 2006.

[16] P. C. Rousé, R. J. Fannin, and D. A. Shuttle, "Influence of roundness on the void ratio and strength of uniform sand," *Géotechnique*, vol. 58, no. 3, pp. 227–231, 2008.

[17] I. Holubec and E. D'Appolonia, *Effect of Particle Shape on the Engineering Properties of Granular Soils. Evaluation of Relative Density and its Role in Geotechnical Projects Involving Cohesionless Soils*, ASTM, West Conshohocken, PA, USA, 1973.

[18] J. Zheng and R. D. Hryciw, "Index void ratios of sands from their intrinsic properties," *Journal of Geotechnical and Geoenvironmental Engineering*, vol. 142, no. 12, pp. 1–10, 2016.

[19] D. Sarkar, D. König, and M. Goudarzy, "The influence of particle characteristics on the index void ratios in granular materials," *Particuology*, vol. 46, pp. 1–13, 2019.

[20] D. Sarkar, M. Goudarzy, D. König, and T. Wichtmann, "Influence of particle shape and size on the threshold fines content and the limit index void ratios of sands containing non-plastic fines," *Soils and Foundations*, 2020.

[21] A. K. H. Kwan and W. W. S. Fung, "Packing density measurement and modelling of fine aggregate and mortar," *Cement and Concrete Composites*, vol. 31, no. 6, pp. 349–357, 2009.

[22] T. L. Youd, "Factors controlling maximum and minimum densities of sands," in *Evaluation of Relative Density and its Role in Geotechnical Projects Involving Cohesionless Soils*, E. Selig and R. Ladd, Eds., pp. 98–112, ASTM International, West Conshohocken, PA, USA, 1973.

[23] P. V. Lade, C. D. Liggio, and J. A. Yamamuro, "Effects of nonplastic fines on minimum and maximum void ratios of sand," *Geotechnical Testing Journal*, vol. 21, no. 4, pp. 336–347, 1998.

[24] Z. Y. Xu, N. Xu, and H. B. Wang, "Effects of particle shapes and sizes on the minimum void ratios of sand," *Advances in Civil Engineering*, vol. 2019, Article ID 5732656, 12 pages, 2019.

[25] B. Bahari, TH. Kim, and W. Hwang, "Nonlinear estimation model of minimum void ratio for sand-silt mixtures," *Marine Georesources&Geotechnology*, 2019.

[26] A. Assadi Langroudi, "Micromechanics of collapse in loess," University of Birmingham, Birmingham, UK, Doctoral dissertation, 2014.

[27] Y. Z. P. Liu, R. Gao, and J. Chen, "Exploring the influence of sphericity on the mechanical behaviors of ballast particles subjected to direct shear," *Granular Matter*, vol. 21, no. 4, 2019.

[28] W. H. Zhou, X. Y. Jing, Z. Y. Yin, and X. Geng, "Effects of particle sphericity and initial fabric on the shearing behavior of soil–rough structural interface," *Acta Geotechnica*, vol. 14, no. 6, pp. 1699–1716, 2019.

[29] C. S. Chang, J.-Y. Wang, and L. Ge, "Modeling of minimum void ratio for sand-silt mixtures," *Engineering Geology*, vol. 196, pp. 293–304, 2015.

[30] C. S. Chang and M. Meidani, "Dominant grains network and behavior of sand-silt mixtures: stress-strain modeling," *International Journal for Numerical and Analytical Methods in Geomechanics*, vol. 37, no. 15, pp. 2563–2589, 2013.

[31] M. L. Hentschel and N. W. Page, "Selection of descriptors for particle shape characterization," *Particle & Particle Systems Characterization*, vol. 20, no. 1, pp. 25–38, 2003.

[32] C. F. Mora and A. K. H. Kwan, "Sphericity, shape factor, and convexity measurement of coarse aggregate for concrete using digital image processing," *Cement and Concrete Research*, vol. 30, no. 3, pp. 351–358, 2000.

[33] H. Wadell, "Volume, shape, and roundness of rock particles," *The Journal of Geology*, vol. 40, no. 5, pp. 443–451, 1932.

[34] K. Shinohara, M. Oida, and B. Golman, "Effect of particle shape on angle of internal friction by triaxial compression test," *Powder Technology*, vol. 107, no. 1-2, pp. 131–136, 2000.

[35] S. Thevanayagam and S. Mohan, "Intergranular state variables and stress-strain behaviour of silty sands," *Géotechnique*, vol. 50, no. 1, pp. 1–23, 2000.

[36] V. C. Xenaki and G. A. Athanasopoulos, "Liquefaction resistance of sand-silt mixtures: an experimental investigation

of the effect of fines," *Soil Dynamics and Earthquake Engineering*, vol. 23, no. 3, pp. 1–12, 2003.
[37] J. Yang and L. M. Wei, "Collapse of loose sand with the addition of fines: the role of particle shape," *Géotechnique*, vol. 62, no. 12, pp. 1111–1125, 2012.
[38] R. K. McGeary, "Mechanical packing of spherical particles," *Journal of the American Ceramic Society*, vol. 44, no. 10, pp. 513–522, 1961.
[39] C. S. Chang, Y. Deng, and Z. Yang, "Modeling of minimum void ratio for granular soil with effect of particle size distribution," *Journal of Engineering Mechanics*, vol. 143, no. 9, Article ID 04017060, 2017.